THE JOURNAL OF PHYSICAL CHEMISTRY B

Article

pubs.acs.org/JPCB

Sensitized Photooxidation of *S*-Methylglutathione in Aqueous Solution: Intramolecular (S.∴O) and (S.∴N) Bonded Species

Piotr Filipiak,*[,†] Gordon L. Hug,[†,‡] Krzysztof Bobrowski,[§] Tomasz Pedzinski,[†] Halina Kozubek,[†] and Bronislaw Marciniak[†]

[†]Faculty of Chemistry, Adam Mickiewicz University, 61-614 Poznan, Poland

[‡]Radiation Laboratory, University of Notre Dame, Notre Dame, Indiana 46556, United States

[§]Institute of Nuclear Chemistry and Technology, 03-195 Warsaw, Poland

ABSTRACT: Nanosecond laser flash photolysis was used to generate sulfur radical cations of the thioether, *S*-methylglutathione (*S*-Me-Glu), via the one-electron oxidation of this thioether by triplet 4-carboxybenzophenone. The purpose of this investigation was to follow the neighboring group effects resulting from the interactions between the sulfur radical cationic sites and nearby lone-pair electrons on heteroatoms within the radical cation, especially the electron lone-pairs on heteroatoms in the peptide bonds. The tripeptide, *S*-Me-Glu, offers several possible competing neighboring group effects that are characterized in this work. Quantum yields of the various radicals and three-electron bonded (both intramolecular and intermolecular) species were determined. The pH dependence of photoinduced decarboxylation yields was used as evidence for the identification of a nine-membered ring, sulfur−nitrogen, three-electron bonded species. The mechanisms of the secondary reactions of the radicals and radical cations were characterized by resolving their overlapping transient-absorption spectra and following their kinetic behavior. In particular, sulfur−oxygen and sulfur−nitrogen three-electron bonded species were identified where the oxygen and nitrogen atoms were in the peptide bonds.

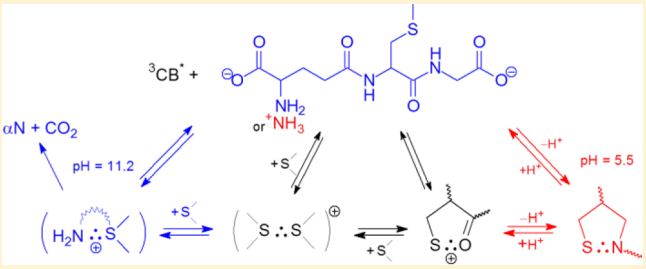

1. INTRODUCTION

S-Alkylglutathiones are naturally occurring oligopeptides in plants, animals and humans.[1] For instance, *S*-methylglutathione (*S*-Me-Glu), the thioether derived from glutathione (GSH), has been found in yeasts,[2] brain tissues,[3] and in *Escherichia coli*.[4] The origin of *S*-Me-Glu is still not understood. However, it is known that yeasts can substitute *S*-methyl cysteine for cysteine in the synthetic pathway of glutathione;[2] GSH can react directly with electrophilic compounds such as methyl bromide;[5] and *S*-Me-Glu synthesis depends on the presence of the chemotaxis methyltransferase and two precursors, glutathione and *S*-adenosyl-methionine.[4] *S*-Me-Glu was also found as a metabolic product in the presence of various methylated drugs and pesticides in animals and plants.[1] *S*-Me-Glu is a common product from the metabolism of methyl halides by glutathione *S*-transferases.[6] The major metabolic pathways for methyl chloride,[7−9] methyl bromide,[6,10,11] and methyl iodide,[6,12,13] in liver, brain, and kidneys of different rodent species and in human erythrocytes are conjugations with GSH to form *S*-Me-Glu.

S-Alkylglutathiones play various functions in living organisms. For instance, *S*-alkylglutathiones act as selective ligands of brain ionotropic glutamate receptors,[14] are inhibitors of the glyoxylase cycle,[15,16] and protect glutathione transferase from inactivation.[17] In addition, *S*-Me-Glu acts as an inhibitor of the reduction of *S*-nitrosoglutathione mediated by alcohol dehydrogenase, albeit substitution of the sulfhydryl proton in GSH with a methyl group hardly improved the inhibitory effect of GSH by itself.[18] Furthermore, it has been shown that *S*-Me-Glu can modulate or regulate responses of the *N*-methyl-D-aspartate glutamate receptor,[19] supports transendothelial fluid transport,[20] and effectively promotes oxidative damage to DNA.[21] Therefore, the oxidative degradation of *S*-alkylglutathiones induced by reactive oxygen species (ROS) and carbonyl triplets (potent oxidizing agents in biological materials)[22] can be relevant to the possible disorders during oxidative stress (for example, see a sample of recent reviews).[23−26]

The *S*-Me-Glu, investigated in the current work, is a tripeptide that contains an *S*-methylcysteine residue with a thioether moiety that is susceptible to attack by oxygen or nitrogen free radicals. We have already investigated the oxidation mechanism of *S*-Me-Glu induced by •OH radicals.[27] The internal *S*-Me-Glu residue (*S*-methylcysteine) was found to be the main target for oxidation. Moreover, it was demonstrated that different intramolecularly three-electron bonded radicals involving sulfur and heteroatoms (N and O atoms) were formed. An intramolecularly (S.∴O)-bonded radical cation is of particular note since it supports our recent observations that sulfur radical cations can be complexed with

Received: December 11, 2012
Revised: January 21, 2013
Published: January 24, 2013

oxygen atoms from the peptide bonds,[28] and thus has biological implications.

There is, however, a key difference in primary products when oxidation occurs by strong one-electron oxidants such as triplet 4-carboxybenzophenone (^{3}CB*) as compared to oxidation by $^\bullet$OH radicals. The quenching of ^{3}CB* by *S*-Me-Glu can lead to the formation of the short-lived radical ion-pair [CB$^{\bullet-}\cdots$>S$^{+\bullet}$], whereas the scavenging of $^\bullet$OH radicals by *S*-Me-Glu can result in the formation of the hydroxysulfuranyl radical (>S$^\bullet-$OH) at the *S*-methylcysteine residue, in analogy with other thioethers. Both of these primary transients decay by several reaction channels which are controlled by the pH of the reaction environment and the presence of neighboring groups.[29]

In this study, we investigated the one-electron oxidation of *S*-Me-Glu by the triplet state of 4-carboxybenzophenone (^{3}CB*) at two pH values (6.5 and 11), in order to unravel the mechanism of the oxidation of the *S*-methylcysteine residue in *S*-Me-Glu. This oligopeptide can also serve as a primary model for protein molecules where, for example, higher-order structures may bring functional groups into close proximity to the thioether group.

2. EXPERIMENTAL SECTION

2.1. Materials. *S*-Methylglutathione (*S*-Me-Glu) was purchased from Sigma (see structure in Chart 1). *S*-Me-Glu (batch no 35H7862) appeared to contain iodide contamination that was removed by recrystallizing *S*-Me-Glu from a mixture of water and acetone before use.

Chart 1

pH = 5.5

S-Me-Glu

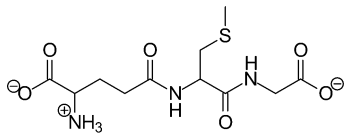

pH = 11.2

S-Me-Glu

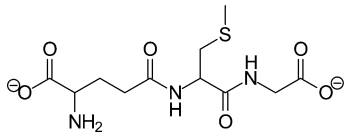

The iodide impurity could have caused serious interference with the monitoring of transient absorption in the visible region of the spectrum. The "crystals" were amorphous, but *S*-Me-Glu solutions purified by this procedure showed no anomalous transient absorption at λ = 360 nm. If iodide had been present, it would have been indicated by the presence of sulfide radical cation−iodide interactions.[30] 4-Carboxybenzophenone (CB) was purchased from Aldrich. The other chemicals were obtained as follows: perchloric acid ($HClO_4$) was purchased from Aldrich Chemical Co. (Milwaukee, WI), and reagent grade NaOH was obtained from J.T. Baker. Acetone (for recrystallizing) was purchased both from Merck and J.T. Baker. HCl (for CO_2 identification) was purchased from Merck. 2-Hexanone and cyclohexane were purchased both from Merck and J.T. Baker.

The deionized water for time-resolved experiments (18 MΩ resistance) was purified in a reverse osmosis/deionization water system from Serv-A-Pure Co. The deionized water for the steady-state analysis came from a water-purification system provided by a Millipore (Simplicity) Co. The pH was adjusted by the addition of either NaOH or $HClO_4$.

2.2. Steady-State Photolysis. Determination of Quantum Yields for Decarboxylation. Steady-state photolysis experiments were carried out in 1 cm × 1 cm rectangular UV cells on a standard optical-bench system. A high-pressure mercury lamp (HBO 200) was used as the excitation source for irradiation. The radiation from this lamp was passed through a combination of glass and interference filters to isolate radiation of wavelength 313 nm. A solution of 2-hexanone in cyclohexane was used as an actinometer.[31]

Irradiation times were chosen to limit conversion of CB to the range 5−40%. Changes in the CB concentration during irradiation were determined spectroscopically at room temperature using both, a Hewlett-Packard 8452A diode array spectrophotometer and a Varian Cary 300 Bio spectrophotometer.

The concentration of CO_2, produced during irradiation, was measured by gas chromatography (GC) in the following fashion. After irradiation, the solutions were acidified with concentrated HCl, and the vapor phase in the reaction cell was analyzed for the presence of CO_2 using a Hewlett-Packard 5890 series II chromatograph. The detection system involved a thermal conductivity detector (TCD) at the end of a Para Plot Q column. Analyses were also performed with HP-HFAP and ULTRA 1 capillary columns (0.32 mm × 25 m) using a temperature program operating between 120 and 220 °C (heating rate, 10 °C/min) and a flow rate of 1.5 mL/min. The CO_2 quantum yields obtained for at least five different irradiation times were then extrapolated to zero irradiation time.

2.3. Laser Flash Photolysis. The nanosecond laser flash photolysis system at the Notre Dame Radiation Laboratory was used for the time-resolved experiments. This data acquisition system has been previously described in detail.[32] Laser excitation at 337.1 nm from a Laser Photonics PRA/Model UV-24 nitrogen laser (operated at about 4−6 mJ, pulse width ≈8 ns) was at a right angle with respect to the monitoring light beam. The detection system consisted of a pulsed xenon lamp (1 kW) as the monitoring light source and a SPEX 270 M monochromator coupled with a Hamamatsu R955 photomultiplier (PMT). The signal from the photomultiplier was processed by a LeCroy 7200 digital storage oscilloscope (OSC 7242 B) and a PC-AT compatible computer (PC). Cut-off filters were used to avoid spurious response from second-order scattering of the monochromator gratings. All experiments were carried out with a gravity-driven flow system and a rectangular quartz optical cell (0.5 × 1 cm). The monitoring-light path length was 0.5 cm. A solution of CB (2 mM) at neutral pH was used as a relative actinometer[33] by monitoring its triplet−triplet absorption (ε_{535} = 6250 M^{-1} cm^{-1}).[34] Typically, 5−10 laser shots were averaged for each kinetic trace. All solutions were deoxygenated by bubbling high-purity argon through them. The reservoir of the flow system typically was loaded with 50−70 mL of solution per transient spectrum.

2.4. Spectral Acquisition and Resolutions of Transient Absorption Spectra. Preliminary to the determination of quantum yields, a set of kinetic traces was collected for a sequence of monitoring wavelengths between 360 and 720 or

dx.doi.org/10.1021/jp312184e | J. Phys. Chem. B 2013, 117, 2359−2368

760 nm at 10-nm intervals. For each individual kinetic trace acquired, the data-acquisition system automatically generates 10 kinetic traces, on 10 distinct time scales. This redundancy of time scales makes it relatively easy to assemble transient spectra at convenient time delays following the laser pulse.

Since there were numerous overlapping optical transients, a spectral-resolution procedure was used.[35] It could be used after the transient spectra were collected and assembled for the relevant time windows. In each chosen time window, the resulting spectra were decomposed into the component spectra associated with the various transient species present via a multiple linear regression method based on the form:

$$\Delta A(\lambda_i) = \sum_j \varepsilon_j(\lambda_i) a_j \quad (1)$$

where ε_j is the molar absorption coefficient of the jth species and the regression parameters, a_j, are equal to the concentration of the jth species times the optical path length of the monitoring light. The sum in eq 1 is over all species present. For any particular time delay of an experiment, the regression analysis included equations such as eq 1 for each λ_i under consideration. The results of this procedure could then be used to produce concentration profiles of the transients with time.

The set of transient intermediates that were likely present were suggested by the intermediates identified in the pulse radiolytic oxidation of *S*-Me-Glu. The reference spectra of these transients have been obtained in previous work.[27] The molar absorption coefficients of the relevant transients, that will be further identified below, are the transients from CB (its triplet-state ^{3}CB* ε_{540} = 6250 M^{-1} cm^{-1}, radical anion $CB^{\bullet-}$ ε_{650} = 7600 M^{-1} cm^{-1}, and ketyl radical $CBH^{\bullet}$ ε_{570} = 5200 M^{-1} cm^{-1}),[34,36] the dimeric (S.∴S)-bonded radical cation ($(S.\therefore S)^+$, λ_{max} = 480 nm and ε_{480} = 6880 M^{-1} cm^{-1}), and the (S.∴O)-bonded radical cation ($(S.\therefore O)^+$, λ_{max} = 400 nm and ε_{400} = 3000 M^{-1} cm^{-1}).[27] Although various $(S.\therefore N)^+$ species were identified, they were incorporated as rescaling certain $(S.\therefore O)^+$ contributions (using λ_{max} = 390 nm and ε_{390} = 4520 M^{-1} cm^{-1}) since the spectra shapes of $(S.\therefore N)^+$ and $(S.\therefore O)^+$ are very similar.[37]

After the transient spectra were assembled, each of these spectra was resolved into component spectra associated with the various transient species deemed to be present. These spectral resolutions were made by fitting the reference spectra to the observed transient spectra via eq 1. With the use of this spectral-resolution technique, concentrations of the transients were determined at any desired time delay following the laser pulse and are displayed as concentration profiles.

2.5. Determination of Quantum Yields. The resulting concentration profiles for the ^{3}CB* quenching experiments at both pH values were extrapolated back to time zero in order to make estimates of the initial quantum yields. Relative actinometry was used with separate cells of CB at a concentration such that the optical densities of the solutions at 337 nm were matched in the CB actinometry cell and the quenching-solution cell. This gave the concentration of the triplet state from which the quantum yields could be calculated as a ratio of concentrations. This is possible because the triplet quantum yield of CB is normally taken to be one.[38]

3. RESULTS AND DISCUSSION

3.1. Radical Processes Following ^{3}CB* Quenching by *S*-Me-Glu at pH 11.2. Figure 1 shows the transient absorption spectra obtained at different delay times after the laser pulse in Ar-saturated solutions containing 20 mM of *S*-Me-Glu and 2 mM of CB at pH 11.2.

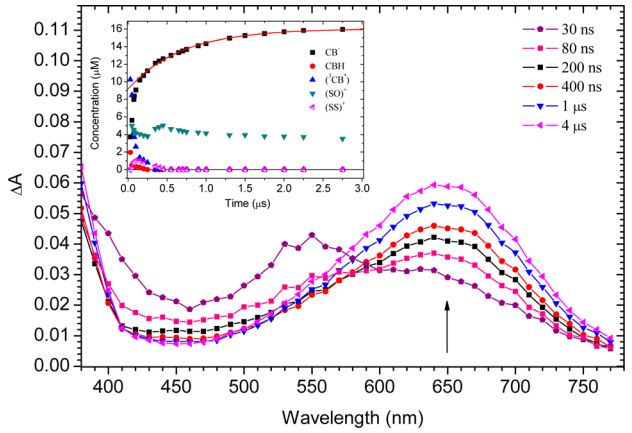

Figure 1. Transient absorption spectra (337-nm laser flash photolysis) following triplet quenching of CB by *S*-Me-Glu (20 mM). CB (2 mM), in Ar-saturated aqueous solution, pH = 11.2, relative actinometry: [^{3}CB*] = 19.3 μM. Inset: concentration profiles of product formation following the triplet quenching of CB by *S*-Me-Glu.

There is a broad absorption band in the 450−750 nm range with λ_{max} = 640 nm and a weaker second absorption band with λ_{max} = 550 nm. The weaker absorption band decayed quite rapidly (within 200 ns). The 550 nm transient was attributed to the triplet-state absorption of CB. After ca. 200 ns, the transient absorption spectrum was dominated by the 640-nm band. This 640 nm band grew in for ca. 4 μs and decayed only about 10% over the remainder of the observation time (150 μs after the pulse). For chemical reasons, it was anticipated (and supported by findings described below) that the broad absorption spectrum with λ_{max} = 640 nm represents practically only one species, which is attributed to the CB radical anion. In addition, two or three species were found to be present in the region of 400−500 nm. These additional species were the dimeric (S.∴S)-bonded radical cation and the (S.∴O)-bonded radical cation (see the inset to Figure 1).

However, there was some uncertainty in the identity of the species responsible for the 390-nm absorption band. After ca. 500 ns, the species is assigned to the (S.∴O)-bonded radical cation. However, the rapid decay, occurring in the time preceding about 500 ns, must be due to some other species, most likely an (S.∴N) species which are known to have very similar absorption spectra to those of $(S.\therefore O)^+$ radical cations. Lifetimes of (S.∴N)-bonded radical cations have also been observed to be of this order of magnitude in basic solutions.[39] The most likely candidate for the (S.∴N)-bonded radical cation is the 9-membered ringed species (Chart 2), whose presence at this pH is based on other evidence which is discussed below or possibly a 5-membered (S.∴N)-bonded species (Chart 2).

From the concentration profile in the inset to Figure 1, several important quantitative yields and rates can be determined. Using the concentration of triplets from relative actinometry, the concentrations in the inset to Figure 1 were used to compute quantum yields. In this manner, it was determined that the initial quantum yield for CB radical anions was equal to 0.55, following a fast growth. As can be seen in the concentration profile in the inset to Figure 1, there is also a secondary, slow, growth of $CB^{\bullet-}$. The total quantum yield

dx.doi.org/10.1021/jp312184e | J. Phys. Chem. B 2013, 117, 2359−2368

Chart 2

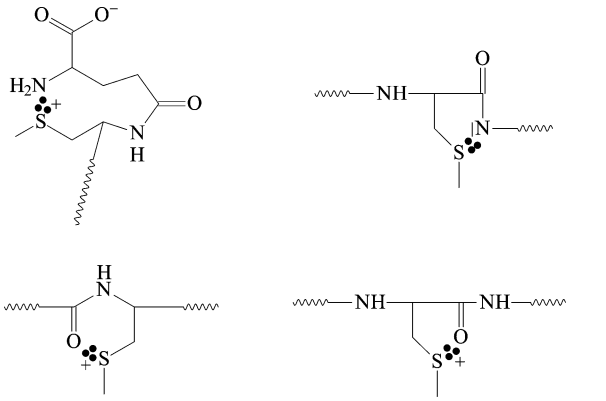

(asymptotic value) after this slow growth was calculated to be 0.82. Ignoring the first 500 ns of the $(S.^{\cdot}.O)^+$ concentration profile as probably due to the 9-membered ring $(S.^{\cdot}.N)^+$, the $(S.^{\cdot}.O)^+$-bonded 5- or 6-membered ring radical cation (Chart 2) reaches a quantum yield of 0.28 (which is further explained below).

Although the 6-membered ring in $(S.^{\cdot}.O)^+$ radical cations is thermodynamically favorable, its formation cannot compete kinetically either with the formation of 5-membered rings in $(S.^{\cdot}.O)^+$ radical cations or with deprotonation of sulfur radical cations to form α-(alkylthio)alkyl radicals.[27] The relative ease of these competitions were demonstrated in experiments which substituted the *S*-methylcysteine residue in *S*-Me-Glu with a methionine residue to form the tripeptide γ-Glu-Met-Gly.[27] In the oxidized *S*-Me-Glu, there was a substantial absorbance in the spectral region around 390 nm which is characteristic[27,37,40] of $(S.^{\cdot}.O)$ radicals and $(S.^{\cdot}.O)^+$ radical cations (potentially either 5- or 6-membered rings for this particular radical cation). In contrast, in the oxidized γ-Glu-Met-Gly, there was a substantial decrease of absorbance in this spectral region where any $(S.^{\cdot}.O)^+$ radical cations with a 6-membered ring should have absorbed. Instead, there was an increase in the region of 490 nm where dimeric $(S.^{\cdot}.S)^+$ radical cations absorb and in the region of 290 nm where α-(alkylthio)alkyl radicals absorb. The conclusions[27] were that the 390-nm absorption in oxidized *S*-Me-Glu was the $(S.^{\cdot}.O)^+$ radical cation with a 5-membered ring, and that formation of a 6-membered $(S.^{\cdot}.O)^+$ radical cation (in γ-Glu-Met-Gly) could not compete with the formation of the other radicals mentioned above in this paragraph. As a further indication of the slowness of the formation of the 6-membered $(S.^{\cdot}.O)$-type radicals, no absorptions which can have been assigned to them were observed in 4-methylthiobutanol aqueous solutions after photooxidation using ^{3}CB*.[41]

In addition to these quantum yields calculated above, the concentration profiles give kinetics information on the reactive intermediates. There is a growth and decay of intermolecularly $(S.^{\cdot}.S)$-bonded radical cations with a decay lifetime of about 0.15 μs. The very fast decay of the ketyl radicals ($CBH^{\bullet}$) was fitted to an exponential decay with a lifetime of about 100 ns and was assigned to their deprotonation to ketyl radical anions ($CB^{\bullet-}$). As mentioned above, fast decay of the 390 nm absorbance (with a lifetime 5.5 μs) at this pH can be assigned to the decay of the 9-membered ring $(S.^{\cdot}.N)^+$ on the basis of other evidence below and/or a 5-membered $(S.^{\cdot}.N)$-bonded species (Chart 2). The nitrogen atoms in the peptide bonds do initially form primarily $(S.^{\cdot}.NH)^+$ radical cations, but they further deprotonate giving $(S.^{\cdot}.N)$-bonded radicals.[28]

3.2. Radical Processes Following ^{3}CB* Quenching by *S*-Me-Glu at pH 5.5. Figure 2 shows the transient absorption spectra obtained at different delay times after the laser pulse in Ar-saturated solutions containing 20 mM of *S*-Me-Glu and 2 mM of CB at pH 5.5.

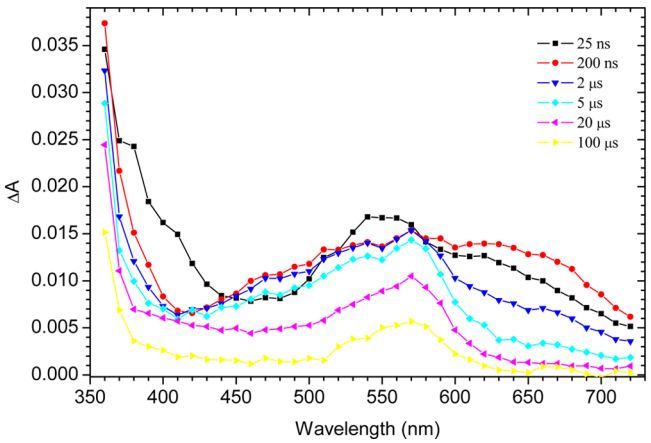

Figure 2. Transient absorption spectra (337-nm laser flash photolysis) following triplet quenching of CB by *S*-Me-Glu (20 mM). CB (2 mM), in Ar-saturated aqueous solution, pH = 5.5, relative actinometry: $[^3CB^*]$ = 7.1 μM.

It exhibits a broad absorption band in the 410−720 nm range with λ_{max} = 570 nm and a slightly weaker second absorption band with λ_{max} = 660 nm. The weaker absorption band decayed with a lifetime of τ_{650} = 2.6 μs. The transient species responsible for this absorption was assigned as the CB radical anion. The triplet state of CB decayed much faster. However, because its absorption overlapped with the $CBH^{\bullet}$ radical's absorption band, the triplet decay parameter could not be determined accurately under these conditions. After ca. 5 μs following the laser pulse, the transient absorption spectrum was dominated by the 570-nm band with a lifetime of about 40 μs. For chemical reasons, it was anticipated (and supported by findings described below) that the broad absorption spectrum with λ_{max} = 570 nm represents practically only one species, which is the $CBH^{\bullet}$ radical.

It was also found that, at least, two additional species were present in the spectral region of 380−500 nm. The two species were the dimeric $(S.^{\cdot}.S)$-bonded radical cations, and the $(S.^{\cdot}.O)$-bonded radical cations (see Figure 3). Their presence came from investigations involving spectral resolutions. However, we could not assign definitely the species responsible for rapid decay of the 390-nm absorption band. We presume that after ca. 6 μs, the $(S.^{\cdot}.O)$-bonded 5-membered ring radical cation is responsible for this absorption band.

But prior to that time, the species may be a 9-membered ring $(S.^{\cdot}.N)$-bonded radical cation and/or a 5-membered $(S.^{\cdot}.N)$-bonded radical (Chart 2) because these species have very similarly shaped absorption bands[37] differing mainly in that their molar absorption coefficients are approximately 1.5 times higher than those of $(S.^{\cdot}.O)^+$. Generally, it is possible to form an $(S.^{\cdot}.N)^+$ with a 9-membered ring via a two-step process: proton transfer from the protonated amino group of the S-centered radical cation to the $CB^{\bullet-}$ within the initially formed radical ion pair[42] and then formation of $(S.^{\cdot}.N)^+$. This

dx.doi.org/10.1021/jp312184e | J. Phys. Chem. B 2013, 117, 2359−2368

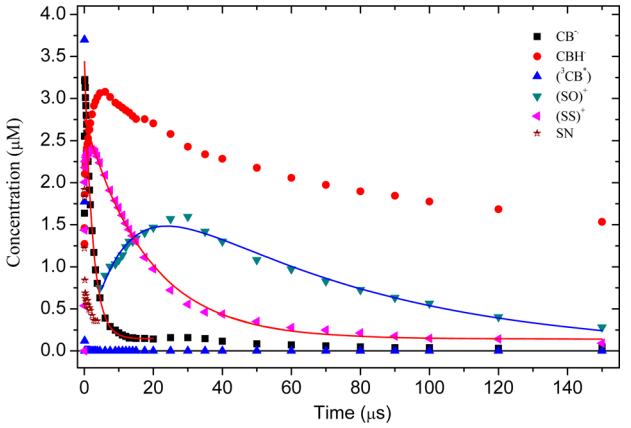

Figure 3. Concentration profiles of product formation following triplet quenching of CB by *S*-Me-Glu (20 mM). CB (2 mM), in Ar-saturated aqueous solution, pH = 5.5, relative actinometry: $[^3CB^*] = 7.1\ \mu M$.

mechanism is inefficient at pH 5.5 because there is no decarboxylation (see Section 3.6) or dark reaction (see Section 3.4) at this pH (see below), and both of these observations are attributed to a precursor radical, $(S\therefore N)^+$ with a 9-membered ring at pH 11.2 (see Section 3.8). Another possibility for an $(S\therefore N)$-bonded species is a 5-membered ring using the lone pairs on the nitrogen of the peptide link between the S-methylcysteine and the glycine residues (Chart 2). This and other possibilities are discussed below in the mechanistic section.

From the concentration profiles in Figure 3, quantum yields and kinetics can be determined that are relevant to the primary and secondary events of the $^3CB^*$ photoinduced oxidation of *S*-Me-Glu at pH 5.5. The initial quantum yield of $CB^{\bullet-}$ was calculated to be 0.48; no secondary growth in the concentration profile of $CB^{\bullet-}$ was seen at pH 5.5, in contrast to its secondary growth seen at pH 11.2, described above. The $(S\therefore O)$-bonded 5-membered-ring radical cations reached a maximum $\Phi = 0.24$. The initial rapid decay was likely due to an $(S\therefore N)$ with a five-membered ring (Chart 2) as mentioned above. The intermolecularly $(S\therefore S)$-bonded radical cations decayed with a lifetime of about 18 μs. The $(S\therefore O)$-bonded 5-membered-ring radical cation formed with the growth rate constant equal to $8.7 \times 10^4\ s^{-1}$. After that growth, this radical decayed relatively slowly with a lifetime equal to 62 μs. The ketyl radical concentration grew and decayed with a maximum in its concentration occurring after about 7 μs. The kinetics of these sulfur-centered radicals are simulated below to support these assignments.

3.3. Rate Constant for Quenching of $^3CB^*$ by *S*-Me-Glu. The rate constant for the quenching of $^3CB^*$ by *S*-Me-Glu was measured by varying the concentration of *S*-Me-Glu and fitting the decay trace of the triplet−triplet absorption of $^3CB^*$ at 535 nm to single-exponential decays. The equation describing the pseudo-first-order decay is

$$k_{obs} = \tau_0^{-1} + k_q[S\text{ - Me - Glu}] \quad (2)$$

where k_{obs} is the reciprocal of the observed triplet lifetime coming from single-exponential fits to the 535-nm kinetic traces, τ_0 is the triplet lifetime of $^3CB^*$ in the absence of quencher, and k_q is the second-order rate constant for the quenching of the triplet by the quencher, *S*-Me-Glu. The resulting rate constants of $(1.0 \pm 0.1) \times 10^9\ M^{-1}\ s^{-1}$ (at pH 5.8) and $(1.0 \pm 0.2) \times 10^9\ M^{-1}\ s^{-1}$ (at pH 11.2) are quite large which is suggestive of triplet-state quenching via electron transfer.

3.4. Characterization of Dark Reaction at pH 11.4. The kinetics and the yield of the secondary reaction at pH 11.4 for the slow growth in absorption at 650 nm were measured. Since the growth rate was dependent on [CB], its pseudo-first-order rate constants, k_{obs}, were determined from kinetic traces such as that in the inset to Figure 4 (secondary growth: $k_{obs} = 1.4 \times 10^6\ s^{-1}$) at a series of CB concentrations.

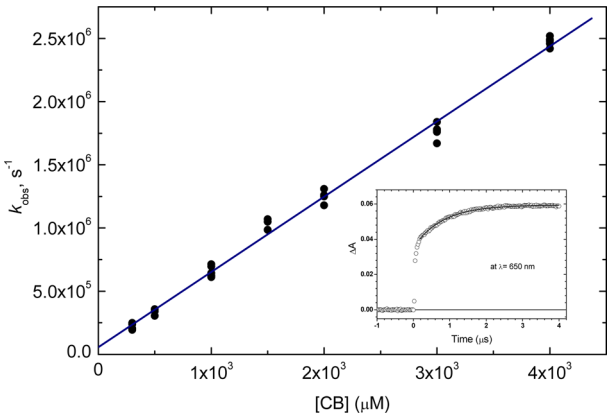

Figure 4. CB concentration dependence of the pseudo-first-order rate constant k_{obs} for the reaction of CB ground state with α-amino-alkyl radical derived from *S*-Me-Glu; (flash photolysis in aqueous solution, pH = 11.4; [*S*-Me-Glu] = 20 mM) Inset: a kinetic trace for the growth of radical anion $CB^{\bullet-}$ formation observed at 650 nm, for [CB] = 2 mM.

The bimolecular rate constant $((6.0 \pm 0.1) \times 10^8\ M^{-1}\ s^{-1})$ for the reduction of CB was determined from the slope of a plot of k_{obs} versus [CB] in Figure 4 for pH 11.4. (In the mechanism section, the reducing agent is suggested to be the αN (α-amino alkyl) radical.) The quantum yield of the secondary amount of $CB^{\bullet-}$ was determined by actinometry from kinetics traces at 650 nm (see inset to Figure 4) or from the concentration profile in the inset to Figure 1. This secondary quantum yield was determined to be $\Phi = 0.27$ (see inset in Figure 4 for example) with the total quantum yield of $CB^{\bullet-}$ determined to be $\Phi = 0.82$.

3.5. Kinetics Simulations. As a preliminary check on whether the assignments of the transients and their kinetics (except for $(S\therefore N)$-bonded radicals (Chart 2)) in Figure 3 are in reasonable agreement with the mechanism to be proposed below for pH 5.5, simulations were run on the following abbreviated scheme for the sulfur-centered radicals. This part of the secondary reaction mechanism was also proposed as part of the reaction scheme following pulse radiolysis *S*-Me-Glu.[27]

$$S^{+\bullet} \rightleftharpoons (S\therefore O)^+ \quad (3)$$

$$S^{+\bullet} + >S \rightleftharpoons (S\therefore S)^+ \quad (4)$$

$$(S\therefore S)^+ \rightleftharpoons (S\therefore O)^+ \quad (5)$$

$$S^{+\bullet} \rightarrow \alpha S \quad (6)$$

Simulations were run with the Chemical Kinetics Simulator software that is free software available from IBM. It was possible to get the simulations, shown in Figure 5, that correspond quite well with the kinetics fittings of the

dx.doi.org/10.1021/jp312184e | J. Phys. Chem. B 2013, 117, 2359−2368

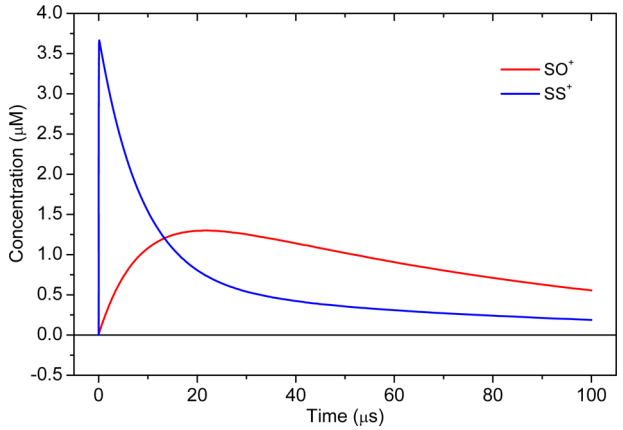

Figure 5. Simulation of the kinetics scheme in reactions 3, 4, 5, and 6 for pH = 5.5 solutions of *S*-Me-Glu quenching of ^{3}CB*.

concentration profiles in Figure 3 for time scales longer than 5 μs after which the (S.∴N)-bonded radicals had disappeared.

The simulation was made with the rate constants for the forward and reverse reactions 3, 1×10^5 and 1×10^4 s^{-1}, respectively; for reactions 4, 2×10^9 M^{-1} s^{-1} and 1×10^6 s^{-1}, respectively; for reactions 5, 5×10^4 and 2×10^4 s^{-1}. Finally, the rate constant for reaction 6 was simulated to be 2×10^6 s^{-1}. The simulated kinetic traces for the decay of the (S.∴S)-bonded radical cation, and for the growth and decay of the (S.∴O)-bonded 5-membered-ring radical cations (see Figure 5) match, qualitatively, to the real concentration profile traces obtained for quenching of ^{3}CB* by *S*-Me-Glu at pH = 5.5 (see Figure 3).

Using time-resolved ESR detection, Yashiro et al.[43] found no evidence for (S.∴O)-bonded 5- or 6-membered-ring radical cations in methionine or *N*-acetyl methionine, whereas such transient species had been previously identified following pulse radiolysis of the derivatives (*N*-acetylmethionine amide and *N*-acetylmethionine methyl ester) using detection by optical and conductivity methods.[44]

3.6. pH-Dependence of Decarboxylation Quantum Yields. Steady-state photolysis experiments were employed to determine the quantum yields for decarboxylation of the ^{3}CB* sensitized oxidation of *S*-Me-Glu for different pH values (see Figure 6). The results indicate that there was no decarboxylation for low pH (6–7), but the quantum yields for CO_2 started increasing at basic pH and reached 0.23 at high pH. These results correlate with the protonation/deprotonation processes of the amino group having a pK_a = 8.7 in the N-terminal γ-Glu residue of *S*-Me-Glu.

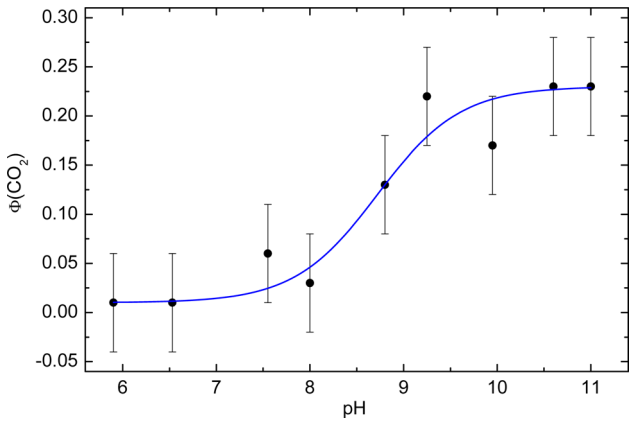

Figure 6. pK_a determination following quantum yields for decarboxylation of *S*-Me-Glu in the steady-state photolysis at 313 nm in aqueous solution varying the pH of the solutions ([CB] = 2 mM, [*S*-Me-Glu] = 13 mM).

3.7. Mechanisms (Primary Reaction). The primary products were very similar following the ^{3}CB* sensitized oxidation of *S*-Me-Glu at both pH 5.5 and 11.2. In both cases, it can be inferred that S-centered radical cation sites were formed in *S*-Me-Glu because of the complementary high yields of radical anions $CB^{\bullet-}$ (see Table 1).

It is plausible that the S-centered radical sites were not seen in the laser flash experiments because their absorption (λ_{max} = 285 nm for $[(CH_3)_2S.\therefore OH_2]^+$)[45] was masked by the ground state absorption of CB and/or that their decay was too rapid. These rationalizations are analogous to the observations and interpretations of the corresponding pulse radiolysis experiments.[27,46] In the proposed mechanism for the quenching of ^{3}CB* by *S*-Me-Glu (see Schemes 1 and 2), the first step is an electron transfer from the sulfur atom in the quencher to the carbonyl group of ^{3}CB*. The result is a pair of radicals, one the radical anion of CB and the other radical being a *S*-Me-Glu with a cationic radical site on the sulfur. That intermediate radical pair can decay via four different pathways: (1) back electron transfer (k_{bt}), (2) charge separation (k_{sep}), (3) proton transfer (k_H), and (4) electron transfer coupled with an amino-group proton transfer (k_{NH}).[42] Pathway (4) does not apply at high pH since the amino group is not protonated.

3.8. Mechanism (at High pH, Secondary Reactions). At high pH (see Scheme 1, pH = 11.2), the main primary product observed was the CB radical anion with an initial quantum yield of 0.55. In aqueous solution, $CB^{\bullet-}$ is in equilibrium with protons and ketyl radicals. However, at this pH, a low concentration of ketyl radicals was observed. The ketyl radicals that escaped from the reaction complex were apparently deprotonated rapidly at pH 11.2. However, there was a secondary reaction of $CB^{\bullet-}$, seen as a slow growth. This reaction is discussed below in connection to the fate of the sulfur radical cations.

In the mechanism (Scheme 1) for pH 11.2, the S-centered radical cationic site on the *S*-Me-Glu is proposed to decay via five different pathways: (1) formation of intramolecularly (S.∴O)-bonded 5-membered-ring radical cations ($\Phi_{primary}$ = 0.28), (2) formation of intermolecularly (S.∴S)-bonded radical cations (Φ < 0.05), (3) formation of intramolecularly (S.∴N)-bonded 9-membered-ring radical cations (Φ = 0.27, see below), (4) possible formation of intramolecular 5-membered (S.∴N)-bonded species, and (5) deprotonation with the formation of αS (α-(alkylthio)alkyl) radicals. As proposed in Scheme 1, the first three reactions involve equilibria. In addition the (S.∴S)-bonded radical cations can form both, (S.∴O)-bonded 5-membered-ring radical cations and (S.∴N)-bonded 9-membered-ring radical cations, via further equilibria.

The evidence for the involvement of (S.∴N)-bonded 9-membered-ring radical cations is of two types, and both are indirect. In analogy to the reaction of the $(S.\therefore N)^+$ radical cation of methionine formed in pulse radiolysis,[47,48] the (S.∴N)-bonded 9-membered-ring radical cations would be expected to decay via fast decarboxylation leading to the formation of the αN (α-amino alkyl) radical. Evidence was found for both of these consequences. First, carbon dioxide was found as a product of the reaction (Figure 6), verifying decarboxylation occurred. Second, a secondary reduction of CB to $CB^{\bullet-}$ was

dx.doi.org/10.1021/jp312184e | J. Phys. Chem. B 2013, 117, 2359–2368

Table 1. Quantum Yields for the Intermediates Formation during Reaction of Quenching CB Triplet by *S*-Me-Glu in Aqueous Solutions

	Φ	
products	pH = 5.5	pH = 11.2
$CB^{\bullet-}$	0.48 (primary)	0.55 (primary); 0.82 (total)
$CBH^{\bullet}$	0.28 (primary)	~0.02 (primary)
SS^{+}	0.34 (max)	<0.05
SO^{+}	0.24 (max)	0.28 (max)
SN^{+} (9-membered ring)	-	0.27[a]
CO_2	<0.02	0.23

[a]Calculated indirectly based on the quantum yield of ketyl radical anion $CB^{\bullet-}$ formed in a dark reaction

Scheme 1. Mechanism at pH = 11.2

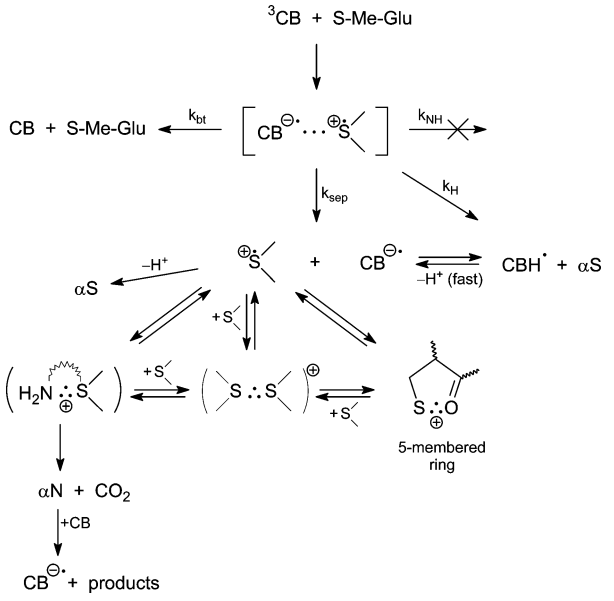

observed (Figure 1 and inset to Figure 4), indirectly supporting the formation of αN radicals, which are known to be reducing radicals (E_{red} = −0.94 V vs SCE).[49] The other potentially reducing radicals (α−(alkylthio)alkyl) were previously found not to be good enough reducing agents to reduce PNAP whereas αN radicals were.[50]

The rationale for the $(S.\therefore N)^+$ species being the intermediate between the sulfur oxidation and decarboxylation can be seen using a resonance theory of the bond. Using *g*-factors from time-resolved ESR, Yashiro et al.[43] computed that the $(S.\therefore N)^+$ bond in oxidized *N*-acetyl methionine at high pH had 40% of the structure $S-N^{+\bullet}$, that is, an oxidizing radical. The participation of such a nitrogen radical cation has also previously[51] been suggested to be the receptor for the transfer of an electron from the ionized carboxyl moiety, with a subsequent decarboxylation in the •OH induced oxidation of γ-Glu-Met.[27]

The *S*-Me-Glu molecule has a single amino group which could form $(S.\therefore N)^+$ radicals with consequent decarboxylation. The other two nitrogens in *S*-Me-Glu are substituted amides which are not easily protonated. Furthermore, any two-centered, three-electron bonds formed with these nitrogens would be $(S.\therefore N)$-bonds[28] which would not likely induce decarboxylation. Scrutiny of the plot of the pH-dependence of $\Phi(CO_2)$ in Figure 6, which has an inflection point at pH 8.7, indicates that the decarboxylation tracked the protonation of the amino group on the γ-Glu residue. When the γ-Glu amino group is deprotonated, its nitrogen lone pairs are available for forming two-centered, three-electron bonds with the sulfur centered radical cation on the *S*-Me-Cys residue. This leads to the formation of an intramolecular $(S.\therefore N)^+$ species with a 9-membered ring, which decays via decarboxylation of the γ-Glu residue. Therefore, it is only the N-terminal amino group of the γ-Glu residue that has a lone pair on its nitrogen which can easily undergo protonation/deprotonation at a pK_a of 8.7. This suggests that the $(S.\therefore N)^+$ intermediate involved in the decarboxylation reaction described is the one with a 9-membered ring.

The second set of the evidence, that is consistent with an $(S.\therefore N)^+$ species being intermediate to the decarboxylation, concerns the observation of a dark reaction (see Figures 1 and 4), forming additional $CB^{\bullet-}$. This is consistent with their being an αN radical that is formed as an immediate consequence of the decarboxylation. Since αN radicals are generally strongly reductive, they can produce the secondary growth of $CB^{\bullet-}$ by a reduction of unreacted CB.

This magnitude of this secondary yield of $CB^{\bullet-}$ is of significance for the support to the proposed reaction scheme. Quantitatively, it matches ($\Phi_{secondary} = 0.82_{total} - 0.55_{primary} = 0.27$), within experimental error, to the quantum yield of decarboxylation at high pH (Φ = 0.23). This is precisely what would be expected from the mechanism where the amount of αN radical should match the amount of CO_2 formed. In addition, because of the pH dependence of the quantum yield for CO_2 formation showing that decarboxylation was coming from the γ-Glu residue, not the Gly residue, again supporting the contention that the $(S.\therefore N)^+$ radical is the species with the 9-membered ring.

3.9. Mechanism (at Low pH, Secondary Reactions). At low pH (see Scheme 2, pH = 5.5) the main primary product was observed to be the CB radical anion with a quantum yield equal to 0.48. At this pH, it decayed via a protonation reaction that can be seen in the concentration profiles in Figure 3. $CBH^{\bullet}$ radicals can be formed by protonations of $CB^{\bullet-}$ either in the reaction complex or the bulk, following the escape of $CB^{\bullet-}$ from the reaction cage.

Complementary with CB radical anion formation, the S-centered radical cationic site on *S*-Me-Glu decays in four different pathways: (1) forming intramolecularly $(S.\therefore O)$-bonded 5-membered ring radical cations (Φ_{max} = 0.24 at 30 μs, see Figure 3), (2) forming intermolecularly $(S.\therefore S)$-bonded radical cations (Φ_{max} = 0.34 at 2.25 μs, see Figure 3), (3) forming αS (α-(alkylthio)alkyl) radicals (Φ = 0.09), and (4) forming a 5-membered $(S.\therefore N)$ species (see below). The first two reactions are equilibrium reactions, but also $(S.\therefore S)$-bonded radical cations can form $(S.\therefore O)$-bonded 5-membered ring radical cations in equilibrium reactions (see Figure 5 and

dx.doi.org/10.1021/jp312184e | J. Phys. Chem. B 2013, 117, 2359−2368

Scheme 2. Mechanism at pH = 5.5

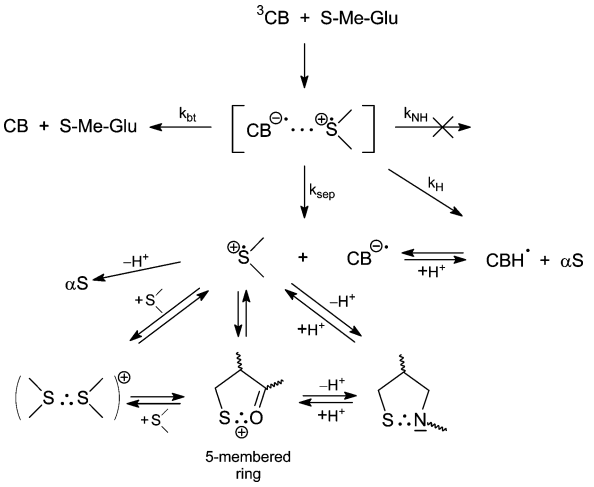

Scheme 2). This part of the reaction scheme that involves the sulfur radicals was simulated in section 3.5, and results are consistent with the rate constants and the experimentally derived concentration profiles.

At pH 5.5, no (S∴N)-bonded 9-membered ring radical cations are expected to be formed directly from the S-centered radical cation because at this low pH, the γ-Glu amino groups have their lone pairs tied up with the protonation and, thus, are not available to form three-electron bonds with the sulfur radical cation. However, the possibility still exists that a 9-membered $(S^{\therefore}N)^+$ species could be formed within the initial radical ion pair (collision complex) through proton transfer from the initially protonated amino group of the S-centered radical cation of *S*-Me-Glu to the $CB^{\bullet-}$ (the k_{NH} reaction step in Scheme 2).[42] The low $\Phi(CO_2) < 0.02$ (see Table 1 and Figure 6) indicates that the 9-membered $(S^{\therefore}N)^+$ was not formed by this mechanism. Therefore, the rapid decay in the concentration profile for the species that had approximately the same spectral shape as the $(S^{\therefore}O)^+$ species, is not the $(S^{\therefore}N)^+$ species with a 9-membered ring.

Another possibility for this rapidly decaying species is a two-centered, three-electron bonded radical formed between the sulfur radical cationic site and the nitrogen in the peptide bond between the *S*-Me-Cys and Gly residues. The lone-pair electrons on this nitrogen heteroatom are more tightly bound than are the lone pairs on the unprotonated (at pH 11.2) amino group of the γ-Glu residue. Thus the likely species initially $(S^{\therefore}NH)^+$ species being formed has tightly held lone pairs which would disfavor the amino radical cationic character in the resonance structure of $(S^{\therefore}NH)^+$ and, as a consequence, would also disfavor electron transfer from the carboxyl group and subsequent decarboxylation, which was not observed at pH 5.5. Furthermore, these types of three-electron bonds, $(S^{\therefore}NH)^+$, would not be very stable and would likely deprotonate to form the (S∴N) radicals (Chart 2) that were found in methionine peptides.[28] Thus, the rapidly decaying species with a 400-nm absorption maximum in Figure 3 is tentatively assigned as such a 5-membered (S∴N) species.

However, based on our photochemical data for *S*-Me-Glu it is not possible to make a definitive assignment at pH 5.5 on whether we are dealing with the protonated or deprotonated form of the (S∴N)-bonded species. Experimental data, including transient conductivity, for *N*-Ac-Met-NH_2,[44] $(Gly)_n$-(Met)-$(Gly)_n$,[44] and cyclo-(L-Met-L-Met) dipeptides[28] suggested a deprotonated form of the (S∴N)-bonded species involving amide nitrogens. On the other hand, theoretical calculations on *N*-Ac-Met-NH_2[52] suggest that the (S∴N)-bonded species involving the amide nitrogen should exist in the protonated form at pH 5.5. However, the question of protonation/deprotonation of the (S∴N)-bonded species involving amide nitrogens is far from being fully understood. For instance, in a time-resolved ESR study[43] of photo-oxidized *N*-Ac-Met anion at pH 12.7, spectral lines were assigned to a protonated (S∴N)-bonded species involving the amide nitrogen. However, these results appear to be in conflict with calculations[52] which suggested a pK_a of 7.2 for $(S^{\therefore}N)^+$/$(S^{\therefore}NH)^+$ equilibrium involving the amide nitrogen of the closely related compound *N*-Ac-Met-NH_2.

4. CONCLUSIONS

Depending on the pH for the quenching reaction of ^{3}CB* by *S*-Me-Glu, different transients were observed, both primary and secondary. To rationalize these mechanistic differences, all the important reaction pathways are shown in Schemes 1 and 2. Substantial differences exist with respect to the secondary reactions. At low pH, no decarboxylation was observed which indicates that the 9-membered ring intramolecular $(S^{\therefore}N)^+$ radical was not formed. At high pH, evidence for this species came from two indirect sources, decarboxylation and a dark reaction. Evidence for the intramolecular, 5-membered ring $(S^{\therefore}O)^+$ species is fairly strong at pH 5.5 and was based both on spectral resolutions and rationalization by kinetics simulations. At low pH, the nature of the short-lived 390 nm transient was ambiguous and may involve the 5-membered (S∴N) species involving a nitrogen in the peptide bond.

AUTHOR INFORMATION

Corresponding Author

*Tel: +48 693 821 974. Fax: +48 61 829 6761. E-mail: piotrf@amu.edu.pl.

Notes

The authors declare no competing financial interest.

ACKNOWLEDGMENTS

This work was supported by COST Chemistry CM0603. This paper is Document No. NDRL 4947 from the Notre Dame Radiation Laboratory which is supported by the Division of Chemical Sciences, Geosciences and Biosciences, Basic Energy Sciences, Office of Science, United States Department of Energy through grant number DE-FC02-04ER15533. G.L.H., B.M., and K.B. thank the NATO Collaborative Research Grants Program for a travel grant (Grant CRG973293). The authors are grateful to Professor K.-D. Asmus for discussions on decarboxylation of radicals.

REFERENCES

(1) Maw, G. A. Biochemistry of *S*-Methyl-L-Cysteine and Its Principal Derivatives. *Sulfur Rep.* **1982**, *2*, 1−32.

(2) Maw, G. A.; Coyne, C. M. The Metabolism of *S*-Methylcysteine in Yeasts. *Arch. Biochem. Biophys.* **1968**, *127*, 241−251.

(3) Kanazawa, A.; Kakimoto, Y.; Nakajima, T.; Sano, I. Identification of γ-Glutamyl Serine, γ-Glutamyl Alanine, γ-Glutamyl Valine and *S*-Methyl Glutathione of Bovine Brain. *Biochim. Biophys. Acta* **1965**, *111*, 90−95.

(4) Terwilliger, T. C.; Bollag, G. E.; Sternberg, D. W.; Koshland, D. E., Jr. *S*-Methyl Glutahione Synthesis Is Catalyzed by the *cheR* Methyltransferase in *Escherichia coli*. *J. Bacteriol.* **1986**, *165*, 958−963.

(5) Grover, P. L.; Sims, P. Conjugation with Glutathione. *Biochem. J.* **1964**, *90*, 603−606.
(6) Hallier, E.; Deutschmann, S.; Reichel, S.; Bolt, H. M.; Peter, H. A Comparative Investigation of the Metabolism of Methyl Bromide and Methyl Iodide in Human Erythrocytes. *Int. Arch. Occup. Environ. Health* **1990**, *62*, 221−225.
(7) IARC In *Monographs on the Evaluation of the Carcinogenic Risk of Chemicals to Humans*; World Health Organization, International Agency for Research on Cancer: Lyon, France, 1986; Vol. *41*, pp 161−186.
(8) Peter, H.; Deutschmann, S.; Reichel, C.; Hallier, E. Metabolism of Methyl Chloride by Human Erythrocytes. *Arch. Toxicol.* **1989**, *63*, 351−355.
(9) Redford-Ellis, M.; Gowenlock, A. H. Studies on the Reaction of Chloromethane with Preparations of Liver, Brain and Kidney. *Acta Pharmacol. Toxicol.* **1971**, *30*, 49−58.
(10) IARC In *Monographs on the Evaluation of the Carcinogenic Risk of Chemicals to Humans*; World Health Organization, International Agency for Research on Cancer: Lyon, France, 1986; Vol. *41*, pp 187−212.
(11) Medinsky, M. A.; Bond, J. A.; Dutcher, J. S.; Birnbaum, L. S. Disposition of ^{14}C Methyl Bromide in Fisher-344 Rats after Oral or Intraperitoneal Administration. *Toxicology* **1984**, *32*, 187−196.
(12) IARC In *Monographs on the Evaluation of the Carcinogenic Risk of Chemicals to Humans*; World Health Organization, International Agency for Research on Cancer: Lyon, France, 1986; Vol. *41*, pp 231−252.
(13) Johnson, M. K. Studies on Glutathione *S*-Alkyltransferase of Rat. *Biochem. J.* **1966**, *98*, 44−45.
(14) Jenei, Z.; Janaky, R.; Varga, V.; Saransaari, P.; Oja, S. S. Interference of *S*-Alkyl Derivatives of Glutathione with Brain Ionotropic Glutamate Receptors. *Neurochem. Res.* **1998**, *23*, 1085−1091.
(15) Elango, N.; Janaki, S.; Rao, A. R. Two Affinity Chromatography Methods for Purification of Glyoxylase-I from Rabbit Liver. *Biochem. Biophys. Res. Commun.* **1978**, *83*, 1388−1395.
(16) Vince, R.; Daluge, S.; Wadd, W. B. Studies on the Inhibition of Glyoxylase I by *S*-Substituted Glutathiones. *J. Med. Chem.* **1971**, *14*, 402−404.
(17) Del Boccio, G.; Pennelli, A.; Whitehead, E. P.; Lo Bello, M.; Petruzzelli, R.; Federici, G.; Ricci, G. Interaction of Glutathione Transferase from Horse Erythrocytes with 7-Chloro-4-nitrobenzo-2-oxa-1,3-diazole. *J. Biol. Chem.* **1991**, *266*, 13777−13782.
(18) Staab, C. A.; Hellgren, M.; Grafström, R. C.; Höög, J.-O. Medium-Chain Fatty Acids and Glutathione Derivatives as Inhibitors of *S*-Nitrosoglutathione Reduction Mediated by Alcohol Dehydrogenase 3. *Chem.−Biol. Interact.* **2009**, *180*, 113−118.
(19) Regan, R. F.; U.S. Patent 6329430, 2001.
(20) Anderson, E. I.; Wright, D. D. Effects of *S*-Methyl Glutathione, *S*-Methyl Cysteine, and the Concentration of Oxidized Glutathione on Transendothelial Fluid Transport. *Invest. Opthalmol. Visual Sci.* **1980**, *19*, 684−686.
(21) Spear, N.; Aust, S. D. Hydroxylation of Deoxyguanosine in DNA by Copper and Thiols. *Arch. Biochem. Biophys.* **1995**, *317*, 142−148.
(22) Cilento, G. Generation of Electronically Excited Triplet Species in Biological Systems. *Pure Appl. Chem.* **1984**, *56*, 1179−1190.
(23) Kennedy, G.; Spence, V. A.; McLaren, M.; Hill, A.; Underwood, C.; Belch, J. J. F. Oxidative Stress Levels Are Raised in Chronic Fatigue Syndrome and Are Associated with Clinical Symptoms. *Free Radical Biol. Med.* **2005**, *39*, 584−589.
(24) Schöneich, C. Methionine Oxidation by Reactive Oxygen Species: Reaction Mechanisms and Relevance to Alzheimer's Disease. *Biochim. Biophys. Acta* **2005**, *1703*, 111−119.
(25) Halliwell, B. Oxidative Stress and Cancer: Have We Moved Forward? *Biochem. J.* **2007**, *401*, 1−11.
(26) Boškovic, M.; Vovk, T.; Plesničar, B. K.; Grabnar, I. Oxidative Stress in Schizophrenia. *Curr. Neuropharmacol.* **2011**, *9*, 301−312.
(27) Bobrowski, K.; Hug, G. L.; Pogocki, D.; Marciniak, B.; Schöneich, C. Sulfur Radical Cation-Peptide Bond Complex in the One-Electron Oxidation of *S*-Methylglutathione. *J. Am. Chem. Soc.* **2007**, *129*, 9236−9245.
(28) Bobrowski, K.; Hug, G. L.; Pogocki, D.; Marciniak, B.; Schöneich, C. Stabilization of Sulfide Radical Cations through Complexation with the Peptide Bond: Mechanisms Relevant to Oxidation of Proteins Containing Multiple Methionine Residues. *J. Phys. Chem. B* **2007**, *111*, 9608−9620.
(29) Bobrowski, K.; Houée-Levin, C.; Marciniak, B. Stabilization and Reactions of Sulfur Radical Cations: Relevance to One-Electron Oxidation of Methionine in Peptides and Proteins. *Chimia* **2008**, *62*, 728−734.
(30) Hiller, K.-O.; Asmus, K.-D. Tl^{2+} and Ag^{2+} Metal-Ion-Induced Oxidation of Methionine in Aqueous Solution. A Pulse Radiolysis Study. *Int. J. Radiat. Biol. Relat. Stud. Phys., Chem. Med.* **1981**, *40*, 597−604.
(31) Murov, S. L.; Carmichael, I.; Hug, G. L. *Handbook of Photochemistry*; 2nd ed.; Dekker: New York, 1993.
(32) Thomas, M. D.; Hug, G. L. A Computer-Controlled Nanosecond Laser System. *Comput. Chem. (Oxford, U.K.)* **1998**, *22*, 491−498.
(33) Carmichael, I.; Hug, G. L. Triplet-Triplet Absorption Spectra of Organic Molecules in Condensed Phases. *J. Phys. Chem. Ref. Data* **1986**, *15*, 1−250.
(34) Hurley, J. K.; Linschitz, H.; Treinin, A. Interaction of Halide and Pseudohalide Ions with Triplet Benzophenone-4-Carboxylate: Kinetics and Radical Yields. *J. Phys. Chem.* **1988**, *92*, 5151−5159.
(35) Marciniak, B.; Bobrowski, K.; Hug, G. L. Quenching of Triplet States of Aromatic Ketones by Sulfur-Containing Amino Acids in Solution. Evidence for Electron Transfer. *J. Phys. Chem.* **1993**, *97*, 11937−11943.
(36) Hurley, J. K.; Sinai, N.; Linschitz, H. Actinometry in Monochromatic Flash Photolysis: The Extinction Coefficient of Triplet Benzophenone and Quantum Yield of Triplet Zinc Tetraphenyl Porphyrin. *Photochem. Photobiol.* **1983**, *38*, 9−14.
(37) Bobrowski, K.; Holcman, J. Formation and Stability of Intramolecular Three-Electron S∴N, S∴S, and S∴O Bonds in One-Electron-Oxidized Simple Methionine Peptides. Pulse Radiolysis Study. *J. Phys. Chem.* **1989**, *93*, 6381−6387.
(38) Inbar, S.; Linschitz, H.; Cohen, S. G. Quenching, Radical Formation, and Disproportionation in the Photoreduction of 4-Carboxybenzophenone by 4-Carboxybenzhydrol, Hydrazine, and Hydrazinium Ion. *J. Am. Chem. Soc.* **1981**, *103*, 7323−7328.
(39) Hug, G. L.; Marciniak, B.; Bobrowski, K. Acid-Base Equilibria Involved in Secondary Reactions Following the 4-Carboxybenzophenone Sensitized Photooxidation of Methionyl-Glycine in Aqueous Solution. Spectral and Time Resolution of the Decaying $(S{\therefore}N)^+$ Radical Cation. *J. Phys. Chem.* **1996**, *100*, 14914−14921.
(40) Mahling, S.; Asmus, K.-D.; Glass, R. S.; Hojjatie, M.; Wilson, G. S. Neighboring Group Participation in Radicals: Pulse Radiolysis Studies on Radicals with Sulfur-Oxygen Interaction. *J. Org. Chem.* **1987**, *52*, 3717−3724.
(41) Bobrowski, K.; Hug, G. L.; Marciniak, B.; Miller, B. L.; Schöneich, C. Mechanism of One-Electron Oxidation of β-, γ-, and δ-Hydroxyalkyl Sulfides. Catalysis through Intramolecular Proton Transfer and Sulfur-Oxygen Bond Formation. *J. Am. Chem. Soc.* **1997**, *119*, 8000−8011.
(42) Hug, G. L.; Bobrowski, K.; Kozubek, H.; Marciniak, B. Photooxidation of Methionine Derivatives by the 4-Carboxybenzophenone Triplet State in Aqueous Solution. Intramolecular Proton Transfer Involving the Amino Group. *Photochem. Photobiol.* **1998**, *68*, 785−796.
(43) Yashiro, H.; White, R. C.; Yurkovskaya, A. V.; Forbes, M. D. E. Methionine Radical Cation: Structural Studies as a Function of pH Using X- and Q-Band Time-Resolved Electron Paramagnetic Resonance Spectroscopy. *J. Phys. Chem. A.* **2005**, *109*, 5855−5864.
(44) Schöneich, C.; Pogocki, D.; Hug, G. L.; Bobrowski, K. Free Radical Reactions of Methionine in Peptides: Mechanisms Relevant to

β-Amyloid Oxidation and Alzheimer's Disease. *J. Am. Chem. Soc.* **2003**, *125*, 13700−13713.
(45) Chaudhri, S. A.; Göbl, M.; Freyholdt, T.; Asmus, K.-D. A Method to Generate and Study $(CH_3)_2S^{+\bullet}$ Radical Cations. Reduction of DMSO by $H^\bullet$ Atoms in Aqueous $HClO_4$ Solutions. *J. Am. Chem. Soc.* **1984**, *106*, 5988−5992.
(46) Asmus, K.-D.; Bahnemann, D.; Bonifačić, M.; Gillis, H. A. Free Radical Oxidation of Organic Sulphur Compounds in Aqueous Solution. *Faraday Discuss. Chem. Soc.* **1978**, *63*, 213−225.
(47) Hiller, K.-O.; Masloch, B.; Göbl, M.; Asmus, K.-D. Mechanism of the $OH^\bullet$ Radical Induced Oxidation of Methionine in Aqueous Solution. *J. Am. Chem. Soc.* **1981**, *103*, 2734−2743.
(48) Asmus, K.-D.; Göbl, M.; Hiller, K.-O.; Mahling, S.; Mönig, J. S.∴N and S.∴O Three-Electron-Bonded Radicals and Radical Cations in Aqueous Solutions. *J. Chem. Soc., Perkin Trans. 2* **1985**, 641−646.
(49) Hiller, K.-O.; Asmus, K.-D. Formation and Reduction Reactions of α-Amino Radicals Derived from Methionine and Its Derivatives in Aqueous Solutions. *J. Phys. Chem.* **1983**, *87*, 3682−3688.
(50) Bobrowski, K.; Schöneich, C. Decarboxylation Mechanism of the N-Terminal Glutamyl Moiety in γ-Glutamic Acid and Methionine Containing Peptides. *Radiat. Phys. Chem.* **1996**, *47*, 507−510.
(51) Bobrowski, K.; Schöneich, C.; Holcman, J.; Asmus, K.-D. $^\bullet OH$ Radical Induced Decarboxylation of γ-Glutamylmethionine and *S*-Alkylglutathione Derivatives: Evidence for Two Different Pathways Involving C- and N-Terminal Decarboxylation. *J. Chem. Soc., Perkin Trans. 2* **1991**, 975−980.
(52) Brunelle, P.; Schöneich, C.; Rauk, A. One-Electron Oxidation of Methionine Peptides—Stability of the Three-Electron S-N(Amide) Bond. *Can. J. Chem.* **2006**, *84*, 893−904.